Accepted Manuscript

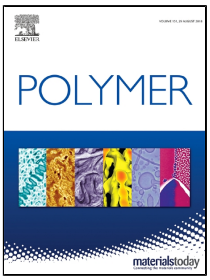

Hydrophobic Esterification of Cellulose Nanocrystals for Epoxy Reinforcement

Binh Minh Trinh, Tizazu Mekonnen

PII:	S0032-3861(18)30822-X
DOI:	10.1016/j.polymer.2018.08.076
Reference:	JPOL 20883
To appear in:	*Polymer*
Received Date:	17 May 2018
Accepted Date:	29 August 2018

Please cite this article as: Binh Minh Trinh, Tizazu Mekonnen, Hydrophobic Esterification of Cellulose Nanocrystals for Epoxy Reinforcement, *Polymer* (2018), doi: 10.1016/j.polymer.2018.08.076

Graphical abstract

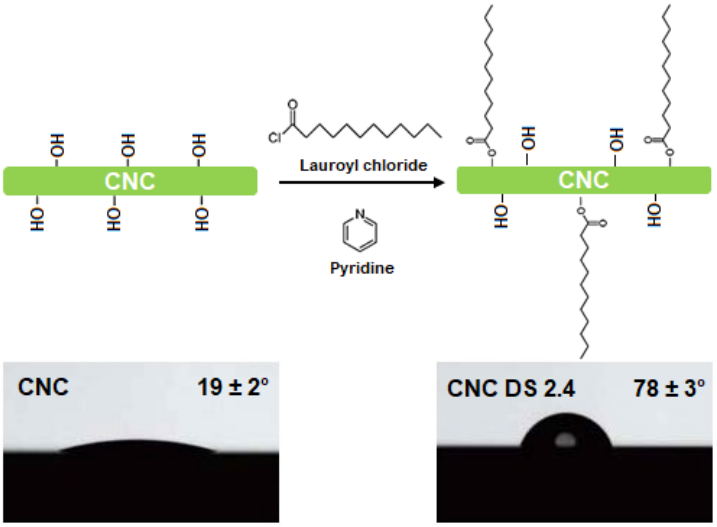

Hydrophobic Esterification of Cellulose Nanocrystals for Epoxy Reinforcement

Binh Minh Trinh, Tizazu Mekonnen*

Department of Chemical Engineering, University of Waterloo, Waterloo, ON, N2L 3G1, Canada

* To whom correspondence should be addressed: tmekonnen@uwaterloo.ca

Abstract

The reinforcing effects of native and modified cellulose nanocrystal (CNC) materials on thermosetting epoxies are investigated. CNC modification is conducted by grafting an activated medium chain fatty acid to substitute the hydroxyl functional group. The level and effect of CNC modification is evaluated using Fourier Transform Infrared (FTIR), elemental analysis (EA), thermal analysis, contact angle measurements, and solvent dispersability studies. The EA shows that CNCs with a degree of substitution (DS) of 0.2, 0.8 and 2.4 is obtained depending on the concentration of the catalyst and reactant used in the process. The native and modified CNCs are then incorporated into epoxy resin via an *in situ* polymerization. Dynamic mechanical analysis, and stress – strain studies showed that the lightly modified CNCs (DS 0.2 and DS 0.8) have an impressive reinforcing effect. CNC with DS 0.2 at 5% loading resulted in a 77% and 44% improvement in the tensile strength and modulus of the baseline epoxy matrix, respectively indicating significant reinforcement. Such materials can be useful in structural composites, printed circuit boards, and adhesive applications. An improvement in the dispersion and an enhanced interfacial adhesion between the modified CNC and the epoxy matrix is proposed for the observed reinforcement. A higher degree of fatty acid grafting onto the CNC resulted in a hydrophobic material, which reduced the water uptake of the epoxy nanocomposites.

Keywords: cellulose nanocrystal (CNC), lauroyl chloride, surface modification, epoxy resins, nanocomposites.

1. Introduction

Epoxy resins are versatile thermosetting polymers characterized by the presence of more than one three-membered oxirane ring. As thermosetting materials, epoxies are highly crosslinked materials and as a result they have high strength, low creep, inherent adhesion, very low shrinkage, excellent corrosion, solvent and weather resistance [1]. Because of these attributes, they are widely used in coatings, structural composites, adhesives and bonding, electrical and electronics, civil engineering, and tooling and castings applications [2]. Nevertheless, the high degree of crosslinking also makes them intrinsically brittle and vulnerable to cracks that limits their applications in important applications such as automotive and aerospace parts manufacture [3][4]. This is due to internal stresses induced during the curing of epoxy, and thus modification is desired to mitigate these drawbacks. The incorporation of nanofillers as a second microphase modifier could be beneficial in this respect. Previous researches have investigated the use of inorganic nanofillers such as metal oxides [5], nanoclays [6], modified clays [7], carbon nanotubes [8], silicon carbide [9], and graphene [3] in epoxies with various degrees of success.

Polysaccharides are prevalent in nature either as a structure forming, essentially insoluble highly aggregated materials (e.g. cellulose), or as water soluble, thickening materials with often various biological functions (e.g. starch, various gums). Structurally, polysaccharides are highly diverse biopolymers composed of repeating glucose units linked via glycosidic bonds. Each repeating unit in the polymer chain has three potentially reactive hydroxyl groups, in most cases one primary and two secondary groups. Based on the polymer's structural characteristics such as linkage of isomers, degree of polymerization, branching, material aggregation and morphology, polysaccharides found various functional uses in polymeric materials. Cellulose nanocrystals (CNCs) derived from cellulose via acid hydrolysis have attracted significant attention in recent

years, because of their natural abundance, relatively low cost, high mechanical strength, and ease of surface functionalization owing to the abundant surface hydroxyl functional groups [10]. Similar to other nanomaterials, CNCs have exceptionally high interfacial area and their structural features are comparable to polymer's molecular size making them appealing reinforcing agents.

The utilization of CNC in composite application is still limited owing to their hydrophilicity, low thermal stability and poor dispersability in mostly non-polar polymers. To achieve optimal load transfer and stress distribution from the matrix to the nanoparticles in nanocomposite structures, efficient dispersion of nanoparticles is essential [11,12]. The aggregation and agglomeration of CNCs in polymer matrices occurs because of the poor interaction between polar CNC and mostly non-polar polymers, and intra- and intermolecular hydrogen bonding between the independent CNC particles. This causes stress concentration and the CNCs act as defects to weaken the effective stress transfer from the fillers to matrix. To mitigate the aggregation and enhance the dispersion of CNCs in polymer matrices, several physical processing techniques (e.g. homogenization, ultrasonication, solid state pulverization, melt mastication etc.)[13,14], and chemical modifications have been investigated.

Chemical modification of CNCs is conducted to improve their dispersion, reduce moisture sensitivity, and improve their interaction with non-polar polymers. The modification includes covalent attachment of molecules [15,16], grafting of polymers on the surface [17,18], surfactant adsorption [18] etc. The grand challenge of CNC chemical functionalization is conducting the reaction in such a fashion that it only changes the surface properties CNCs, while preserving the original morphology and the integrity of the crystal [19] that are important attributes for its use as a reinforcing filler. Here, we present a one-step, robust hydrophobic esterification of CNC with a medium chain acid chloride in an effort to enhance the dispersability and reduce its

hydrophilicity for epoxy nanocomposite applications. The modified CNC is expected to provide effective reinforcement of epoxies together with reduced moisture uptake that are desirable properties in many epoxy applications.

2. Materials and methods

2.1 Materials

Spray dried cellulose nanocrystals (CNC) was obtained from CelluForce Inc (Montreal, Canada). The particle size of the CNC powder, crystalline fraction, sulfur content, and bulk density were 1-50 μm, 88 %, 0.87 %, and 0.7 g/cm^3, respectively. Lauroyl chloride (98%), cesium carbonate (99%), pyridine (≥ 99.0%), toluene (99.9 %), chloroform (99 %), epoxy resin (Araldite 506) and the curing agent poly (propylene glycol) bis (2-aminopropyl ether and were all purchased from Sigma-Aldrich. Ethanol (99%). Acetone (99%) was obtained from Fisher Scientific. CNC was dried at 70 °C for 24 h under vacuum, and kept in a sealed container. All chemicals were used without further purification or modifications.

2.2 Methods

2.2.1 Esterification modification of CNC with acid chloride

As illustrated in scheme 1, an activated fatty acid, lauroyl chloride, was used to modify CNC. Pyridine was used as a catalyst, partial solvent, and acid scavenger. For the esterification reaction, dried CNC was dispersed in toluene (3 wt.%), and homogenized (Homogenizer, PowerGen 700) until a uniform and stable dispersion was obtained. The dispersion was transferred to a three neck round bottom flask for reaction. The reaction flask was then fitted with a condenser and a thermometer and placed in a silicon oil that was set up on a hot plate equipped with magnetic stirring. The dispersion was then heated to 90°C, and a calculated

quantity of lauroyl chloride and catalyst pyridine were added dropwise under agitation. Three levels of lauroyl chloride (5%, 10%, and 20%), and about 2% of pyridine were added to the dispersion similar to a method reported before [20,21] with some modifications. The reaction was then carried out at 110 ^{o}C for 1h under constant stirring. At the end of the 1h reaction time, the suspension was quenched with ethanol, and cooled down to room temperature. The modified CNC product was recovered by washing it with ethanol (three times), followed by acetone (three times), to remove unreacted lauroyl chloride, and the pyridine catalyst. Complete removal of the unreacted lauroyl chloride was confirmed by infrared analysis of the raffinate from the last washing step. The washed product was then dried under vacuum, and stored at room temperature for further analysis.

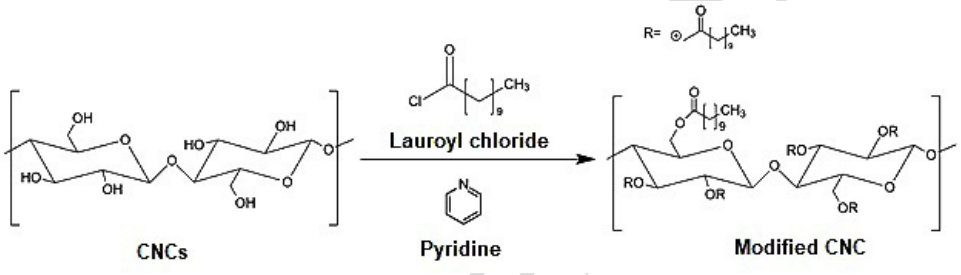

Scheme 1. Reaction of cellulose nanocrystals with lauroyl chloride.

2.3 Characterization of modified CNCs

2.3.1. FTIR spectroscopy

The modification of CNCs were characterized by Fourier Transform Infrared Spectroscopy (FTIR, model Nicolet 6700, Thermo Scientific). For the analysis, about 2 mg of the native and modified CNCs were dried overnight at 80°C and pressed into pellets together with 20 mg potassium bromide (KBr) salt powder. FTIR scans, in transmittance mode, was then gathered in the range between 500 and 4000 cm^{-1} frequency.

2.3.2 Elemental analysis

Elemental analysis was conducted on dried powder samples using a 4010 Elemental Analyzer (Costech Instrument, Italy). Carbon percentages were quantified for native and modified CNC samples in triplicate, and average values were used for calculating the degree of substitution (DS). The DS values for modified CNCs were calculated from the measurement of % C. Calculations of DS value were conducted based on the method proposed by Vaca-Garcia *et al* [22], as shown in equation 1.

$$C = \frac{12.011 \times (6 + \sum DS_i.n_i)}{12.011 \times (6 + \sum DS_i.n_i) + 1.008 \times (6 + \sum 2.DS_i.(n_i - 1)) + 15.999 \times (5 + \sum DS_i)} \quad (1)$$

Where, DS_i is the degree of substitution of the i^{th} carbon chain from lauroyl chloride, and n_i is the number of carbon atoms on each chain. This equation holds true assuming that cellulose has a fixed carbon percentage of 44.44% [22].

2.3.3 X-ray diffraction (XRD)

The analysis of the crystalline structure of the modified CNC powder was carried out with an X-ray Diffractometer D8 Discover (Bruker, Karlsruhe, Germany). The XRD scanning patterns were recorded in a 2θ range from 5 to 55^o with a step size of 0.02^o. The operating condition settings for the diffraction were 40 kV and 40 mA.

2.3.4 Dispersibility of modified CNCs in different organic solvents

The dispersibility of the modified CNCs was studied in various solvents with different polarity. The solvents used in this study were water, ethanol, acetone, tetrahydrofuran (THF), and toluene. Dried powder samples were mixed with the respected solvent and homogenized for

5 minutes. The concentration of each homogenized suspension was kept at 10 mg/mL[16]. The homogenized suspensions were then kept for 12h undisturbed, and sedimentation or floatation was observed visually.

2.3.5. Contact angle measurement

Contact angle measurement of native and modified CNC were carried out on pressed pastille samples. Measurements were conducted at 23°C and 50% relative humidity using a custom-built optical sessile drop system. A deionized water droplet was dropped onto the prepared samples and images were taken after 15s.

2.3.6. Thermogravimetric analysis (TGA)

The impact of fatty acid grafting on the thermal stability of CNC were evaluated by conducting TGA studies on pristine and modified samples. The test was carried out using TA instrument TGA Q500. The dynamic temperature ramp used in this thermal study was 5 ^{o}C/min from 25 to 500 ^{o}C under normal air condition. Thermal degradation behavior was then estimated based on the weight loss against temperature.

2.4. Epoxy biocomposite preparation

Epoxy biocomposites were prepared with both pristine and modified CNCs at loading concentrations of 2.5 and 5 wt. %. Data collected from elemental analysis was used to estimate the equivalent weight of CNC in the modified sample, and composite loadings were based on the weight of CNC, taking the incorporated fatty acids into account. The epoxy formulation consisted of 100 parts per hundred (phr) of epoxy and 30 phr curing agent. The epoxy resin was first mixed with the CNC (pristine and modified), and dispersed well using a homogenizer (PowerGen 700). The calculated curing agent was then added to the epoxy – CNC premix. After

obtaining a uniform mix, the samples were degassed at room temperature in a vacuum oven to remove microbubbles that were created during the homogenization process. The degassed samples were then carefully poured into a silicon mold and allowed to cure at 60°C for 12h. The specimens cured as such were post cured at 120 °C for 2h.

2.4.1. Tensile properties

The casted specimens were conditioned at 23 °C and 50% relative humidity for at least 40 h prior to testing. Tensile tests were then conducted in accordance with ASTM D638-14 (Standard Test Method for Tensile Properties of Plastics). Instron (Instron 4302, Norwood, MA, USA) equipped with a load cell of 10 kN at a crosshead speed of 10 $mm.min^{-1}$ was used for this test.

2.4.2. Dynamic mechanical analysis (DMA)

Thermal-mechanical properties of epoxy-CNC composites were studied by using dynamic mechanical analysis using DMA (TA instrument, DMA Q800). The specimens were scanned in a temperature range from 25 to 150 ^oC at a heating rate of 3 ^oC/min. Three-point bend mode with a frequency sweep of 1 Hz under dynamic strain of 0.004% was used for the test. Sample dimensions were 3 × 12 × 55 mm^3.

2.4.3. Differential scanning calorimetry (DSC)

The thermal transition temperature of neat epoxy, and the CNC (pristine and modified) based nanocomposites was evaluated using DSC (DSCQ2000). An accurately weighed sample of about 5 mg was loaded into a DSC pan and scanned from 20 to 200 ^oC at the ramping rate of 10 ^oC /min in a nitrogen atmosphere. An empty aluminum pan was used as a reference for all the scanning measurements.

2.4.4. Scanning electron microscope (SEM)

Scanning electron microscopy images were collected using FEI instrument (Quantum FEG-SEM 250) operated at 20kV. Tensile fractured sample cross-sections were used for SEM morphology analysis. Carbon tape support was used during the imaging.

2.4.5. Water absorption test

The moisture absorption of the baseline epoxy and the CNC (pristine and modified) reinforced composites were studied in accordance with the ASTM D570-98. In this test, four sample specimens per sample were dried to a constant weight (W_1). The dried specimens were then submerged in deionized water at room temperature, and weight changes were recorded every 24h for seven days. After every 24h of soaking, the extra water on the surface of samples were wiped with blotting paper, and weighed (W_2) until the seventh day. The moisture absorption was then calculated by weight difference between the samples submerged in water and dried samples using equation (2):

$$\text{Moisture absorption} = (W_2 - W_1)/W_1 \times 100 \quad (2)$$

3. Results and discussion

3.1. Modifications and degree of substitution characterization

Cellulose nanocrystals prepared with sulphuric acid generally disperses well in water and other polar solvents because of the residual sulfate functionalities. However, their dispersability is quite limited in polymers and other non-polar solvents. Thus, there is a significant interest in the surface modification of cellulose without disrupting the crystalline structure. Previous studies [15, 24] postulated that about 10% of the total –OH in CNC are exposed to the surface while it is in its native crystal form. Since, the glucose monomers on a cellulose chain have three –OH

groups, the maximum degree of substitution that can be achieved is three. Thus, total substitution of the 10% surface –OH groups amount to a DS of 0.3. In this study, one-step grafting of medium chain fatty acid (C12) onto CNC was conducted under heterogeneous conditions. The activated fatty acid chloride, lauroyl chloride, reacted with the alcohol groups of CNC in the presence of a weak base, here pyridine. The pyridine would be protonated by the HCl by product of the reaction [24], and thus could act as an acid scavenger to prevent the hydrolysis of the CNC by the acid.

Table 1 presents the degree of –OH substitution with lauric acid calculated from elemental analysis. Results obtained here show that the DS of the esterified CNCs ranged from 0.2 to 2.4. A lower concentration of lauroyl chloride (and pyridine) resulted in a DS of 0.2 (<0.3), pointing out that there was only surface modification, and the crystalline structure of the CNC was maintained in such conditions. It was evident that the DS increased with increasing concentration of lauroyl chloride and pyridine for a constant CNC (- OH) concentration as observed from the elemental analysis (Table 1). Despite heterogeneous reactions setup (without dissolution of the CNC), higher concentration of lauroyl chloride and pyridine have significantly disrupted the crystalline structure of CNC resulting in an amorphous morphology. The reason for the high DS with the increase in the reactant and catalyst concentration could be associated with the swelling of the CNC with the base catalyst. The swelling would expose –OH functional groups of the CNC that were otherwise hidden in the crystal structure for reaction with the activated fatty acid.

Table 1: Elemental analysis of unmodified and modified CNCs

Samples	C (%)	Degree of Substitution (DS)
CNC	44.4	-
Modified CNC_1	51.1	0.2
Modified CNC_2	61.3	0.8
Modified CNC_3	70.2	2.4

3.2. Fourier transform infrared spectroscopy (FTIR)

To verify the modifications, IR studies were conducted and spectra of the pristine and the modified CNC samples are presented in Figure 1. The native CNC showed IR peaks at 3450 cm^{-1} (-O-H stretching), 2920 cm^{-1} (-C-H stretching), and 897 (β – glycosidic linkages), similar to other studies [15,25,26]. The esterification clearly resulted in the appearance of new IR peaks or the loss of some existing peaks. One of the most notable changes was the presentation of a new vibration peak at 1750 cm^{-1}, attributed to -C=O stretching as a result of the esterification [27]. The emergence of the new ester carbonyl group on the modified samples further confirmed the esterification of CNCs introduced. These ester bond peaks were observed in all modified CNC as shown in Fig. 1, irrespective of the DS. As expected, these peaks were more prominent in the high DS as compared to the low DS samples.

Another evidence of the grafting of lauric acid on CNCs was the introduction of sp^3 alkyl group vibration representing alkane chain in the region of 2800-2900 cm^{-1} [12, 13]. All the modified CNCs contained these grafted alkane chain (CH_2) peak vibrations attributed to the medium fatty acid chain of lauric acid. Moreover, the transmittance intensity of broad hydroxyl

vibration of CNC has reduced progressively with the increase in the degree of substitution indicating the substitution of the –OH with the fatty acid [21]. For the high DS CNC (DS 2.4), the broad –OH band seemed to completely disappear as the grafted alkane chain replaced most of the hydroxyl group of the nanocellulose.

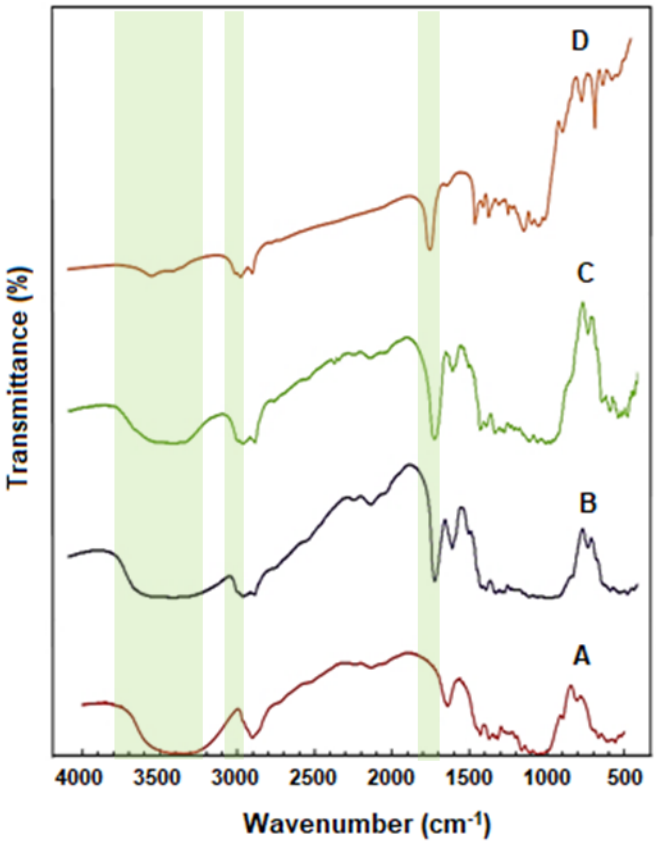

Figure 1. FTIR spectra of native and modified CNCs: (A) Native CNC; (B) Modified CNC, DS 0.2; (C) Modified CNC, DS 0.8; (D) Modified CNC, DS 2.4

3.3. X-ray diffraction

The change in the crystalline structure of CNC with variation in the esterification level was investigated using XRD analysis. The XRD diffraction patterns of native and modified CNCs are displayed in Figure 2. The native CNCs exhibited their distinctive broad peaks (15°, 16.5°), sharp and high peak (23°), and a small peak (35°) similar to other studies [4][6][12]. These peaks at 2θ

of 15°, 16.5°, 23°, and 35° correspond to cellulose I crystallographic planes 110, $\overline{110}$, 200, and 4, respectively [28][29]. A new peak appeared at around 20° in the modified samples. This peak is a small shoulder in DS 0.2 and 0.8 samples (Figure 2b and c). However, in the highly modified CNC samples (DS 2.4), this became a prominent peak (Figure 2d). This peak corresponds to the medium fatty acid chain grafted on the CNC chain [30]. The lightly (DS 0.2) and intermediately (DS 0.8) modified samples (b and c) manifested XRD spectrums that closely resemble the pristine CNC, as they still possess the three main peaks of CNC. Overall, it appeared here that the crystalline structure of CNC were maintained for the lightly and intermediately modified CNCs. However, the highly modified CNC (DS 2.4) displayed a rather weak crystallinity as compared to the other samples. Also, the peaks at around 16, 23, and 35° got progressively weaker with an increase in DS.

It was interesting to notice that the CNC sample with DS of 0.8 maintained the crystallinity as substantiated by the sharp XRD peaks. It is plausible that the lauroyl chloride might not have attacked too deep into the crystalline core of the CNC. Contrarily, all the distinctive peaks of the CNC were no longer observed in the highly modified samples (DS 2.4). Rather, a strong new XRD peak appeared at 20°, which could be attributed to crystallized fatty acid chains [21,25]. XRD diffraction patterns of lauric acid as reported by Kong *et al* [31] also exhibited the manifestation of strong peaks at 2θ of 20° in addition to other peaks. This supports that the prominent peak in the modified CNC (DS 2.4) sample could be a crystal of lauric acid – CNC complex. Overall, the XRD results were in complete agreement with elemental analysis and the IR studies in terms of the level of CNC modification. It can be concluded that the high degree of modification (e.g. in DS 2.4 sample) resulted in delamination of cellulose chains from the packed

crystalline structure. Such reduction of crystallinity could affect the reinforcing capability of CNCs in nanocomposite applications.

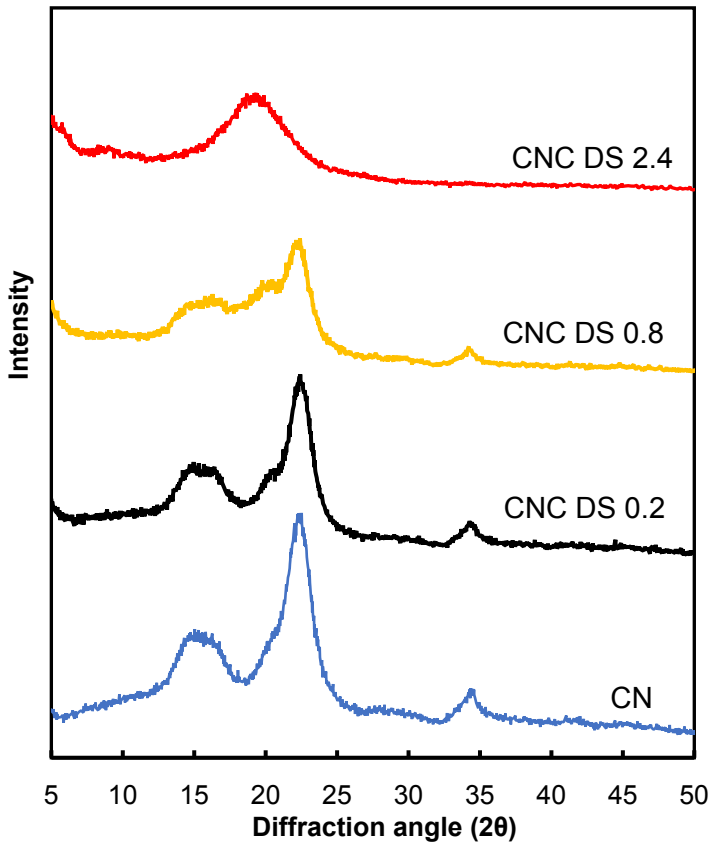

Figure 2. XRD patterns of blank and modified CNC (native CNC, CNC DS 0.2, CNC DS 0.8, and CNC DS 2.4)

3.4. Contact angle measurement

Evaluation of contact angle is among the most established methods for studying the surface properties of materials [32]. The impact of fatty acid modification on the wetting properties of CNCs was invetigated using water contact angle measurement. Figure 3 displays the contact angle (θ) between water droplet and CNC smaples (unmodified and modified). As anticipated, the native CNC gave the lowest contact angle (19°) owing to the hydrogen bonding association

between the –OH groups of CNC and water molecules leading to more dispersion. The contact angle increased with an increase in the degree of substition. In the most modified sample, the contact angle increased to 74°. This is due to the incremental replacement of the polar –OH groups with the non-polar aliphatic chains. This is a clear indication of the reduction in the water wettability, and increase in hydrophobicity of the modified samples as compared to the native CNC. Hu *et al* [15] reported similar trend of contact angle change as a result of surface modification of CNC with natural polyphenols. Espino-Perez *et al* [33] exhibited similar hydrophobicity behavior for carboxylic acid functionalized CNC. Such hydrophobically

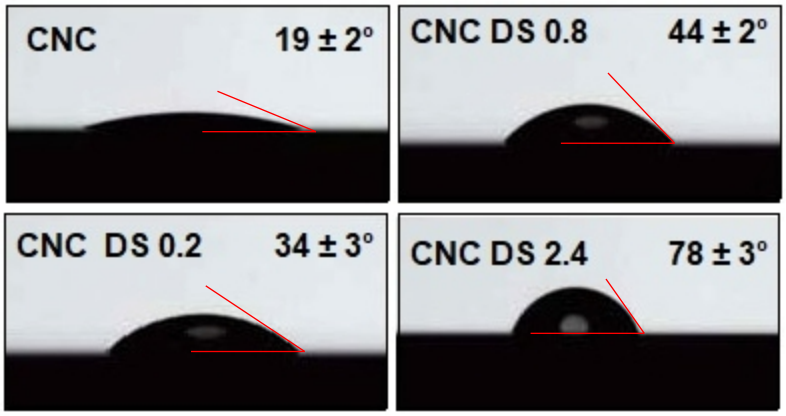

modified CNC are expected to have better dispersibility attribute in nanocomposite applications. Also, their water absorption kinetics would be significantly reduced.

Figure 3. Contact angle of native and modified CNC samples.

3.4. Dispersibility of modified CNCs in organic solvents

Dispersibility test of native and modified CNCs were carried out to demonstrate the hydrophobicity and wettability of CNCs in organic solvents after the esterification modifications. The solvents used for comparison were water (most hydrophilic), ethanol, acetone, THF, and

toluene (most hydrophobic). As shown in Figure 4a, CNC displayed great dispersibility and dispersion stability in water. This was because the residual sulphate anions on CNC accrued from the H_2SO_4 hydrolysis during its production process provided it repulsion force between the particles that led to the observed stable dispersion in water [16,34]. Moreover, the abundant –OH groups of native CNC are available for a strong hydrogen bonding with the water [19,35] to maintain the dispersed state for a fairly extended time. It was noticed that native CNC dispersed relatively well in ethanol as well, but it sedimented by the end of the test (12h) pointing that it has poor dispersion stability. However, with a further increase in the hydrophobicity of the dispersion media, native CNC lost its dispersability. In general, it displayed poor dispersability in THF and toluene.

A dramatic decrease in the dispersibility of modified CNC in water was observed with an increase in the degree of esterification. Lauric acid grafted sample with a DS of 0.8 and 2.4 has shown no sign of dispersability in water as the particles started separating right after the high-power homogenization dispersion. On the contrary, an excellent dispersibility and dispersion stability was observed for the DS 0.8 and DS 2.4 CNC samples in toluene (least polar media), as shown in Figure 4c and 4d. This observation was because the substation of the -OH groups with lauric acid limits CNC – CNC and CNC – water hydrogen bonding interaction. Overall, the modified CNC exhibited an increasing trend of dispersability with increases in their DS and increase in the hydrophobicity of the solvent used. The results observed here are in good agreement with other esterified CNC samples (e.g. acid anhydride, acid chloride, acid catalyzed carboxylic acid, and *in situ* activated carboxylic acid) [16], and also our contact angle study. Improving the dispersibility of CNC in non-polar solvents could be beneficial, as it provides good compatibility with other organic solvent soluble polymers. For instance, the

hydrophobically modified CNC could be easily mixed with hydrophobic polymer matrices, such as such as PP, PE, PCL and PLA, in common organcic solvents. Also, the solvent dispersable easterified CNC can be easily incorporated into epoxy and polyurethane formulations after dispersion in the non-polar solvents. This avoids the laborious task of solvent exchange process e.g. in DMF [35], and acetone [36], that is usually conducted through a series of dispersion and centrifugation process.

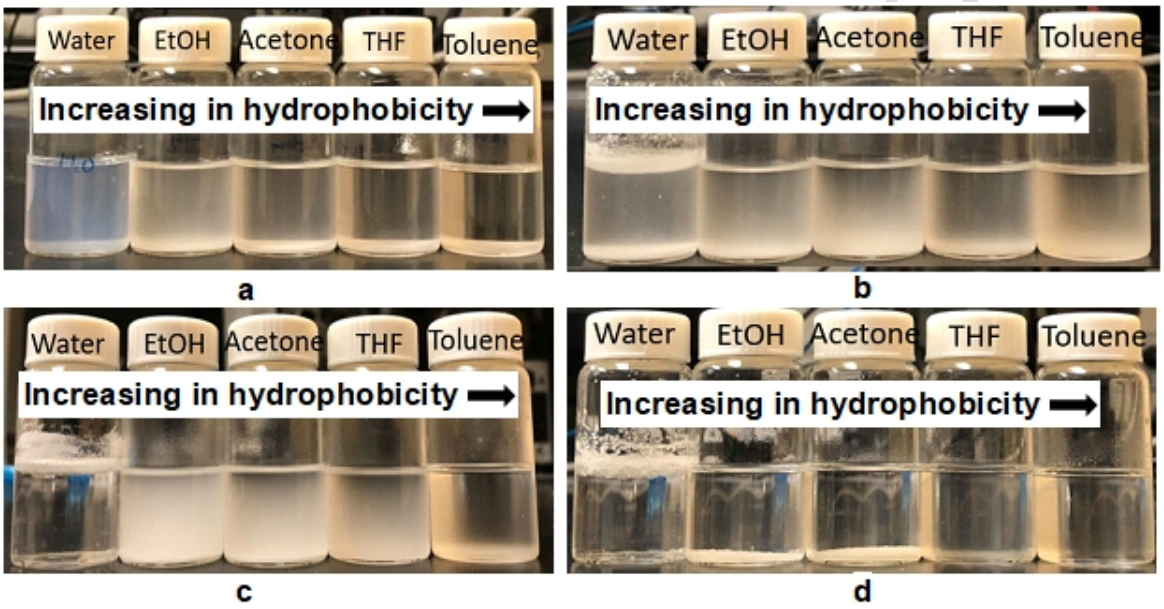

Figure 4. Dispersion of native CNC and modified CNC in different solvents. The concentration of all CNCs in solvents were kept constant at 10 mg/mL. (a) Native CNC; (b) Modified CNC, DS 0.2; (C) Modified CNC, DS 0.8; and (D) Modified CNC, DS 2.4.

3.5. Thermogravimetric analysis (TGA)

Thermal degradation behavior of CNC is a crucial parameter for its use as a filler in polymers. This is because, most plastic processing operations, including melt processing of thermoplastics, compounding of rubber, or curing of epoxy or rubber involve high temperature, and as such the CNC need to stay stabile within the processing regime of polymers. The thermal

stability of the native and esterified CNC samples were evaluated using TGA. Thermograms represented in Figure 5 (a and b) demonstrated that CNC had two principal weight loss regimes at 245°C and 314 °C. Espino-Perez *et al* [33] reported that such two peaks in native CNC could be attributed to the degradation of CNC – SO_4^{2-} (first peak) and CNC-OH (second peak).

Nonetheless, our native CNC sample contained limited sulphate cation (0.87%), and the rather large degradation peaks could not be associated with CNC – SO_4^{2-} degradation. It is plausible that the first peak could be associated with the dehydration of cellulose to dehydrocellulose and second peak could be related to the depolymerisation of CNC and its monomers into volatiles [37,38]. CNC Esterified samples with a DS of 0.2, 0.8 and 2.4 exhibited an onset and peak degradation (in bracket) of 197°C (266°C), 200 °C (274 °C), and 260 °C (305 °C), respectively. The results obtained here indicated that the grafted lauric acid has improved the thermal stability of native CNC irrespective of the degree of substitution. However, the improvement was more pronounced with higher levels of substitution. Also, it was clearly observed that the highly esterified CNC (DS 2.4) exhibited a single peak of degradation. This could be because most of the –OH that was responsible for the dehydration degradation of CNC were already substituted, and as a such a single phase of depolymerisation of both the CNC and the aliphatic chain of the fatty acid could probably have occurred. Overall, native or modified CNC is amenable to polymer processing temperatures, as the thermal degradation point is beyond the melt processing temperature of numerous polymers (e.g., polyethylene, polypropylene, poly(lactic acid), EVA, polyhydroxyl alkanoates etc), or the curing or processing temperature needed in most rubber, unsaturated polyester or epoxy thermosets.

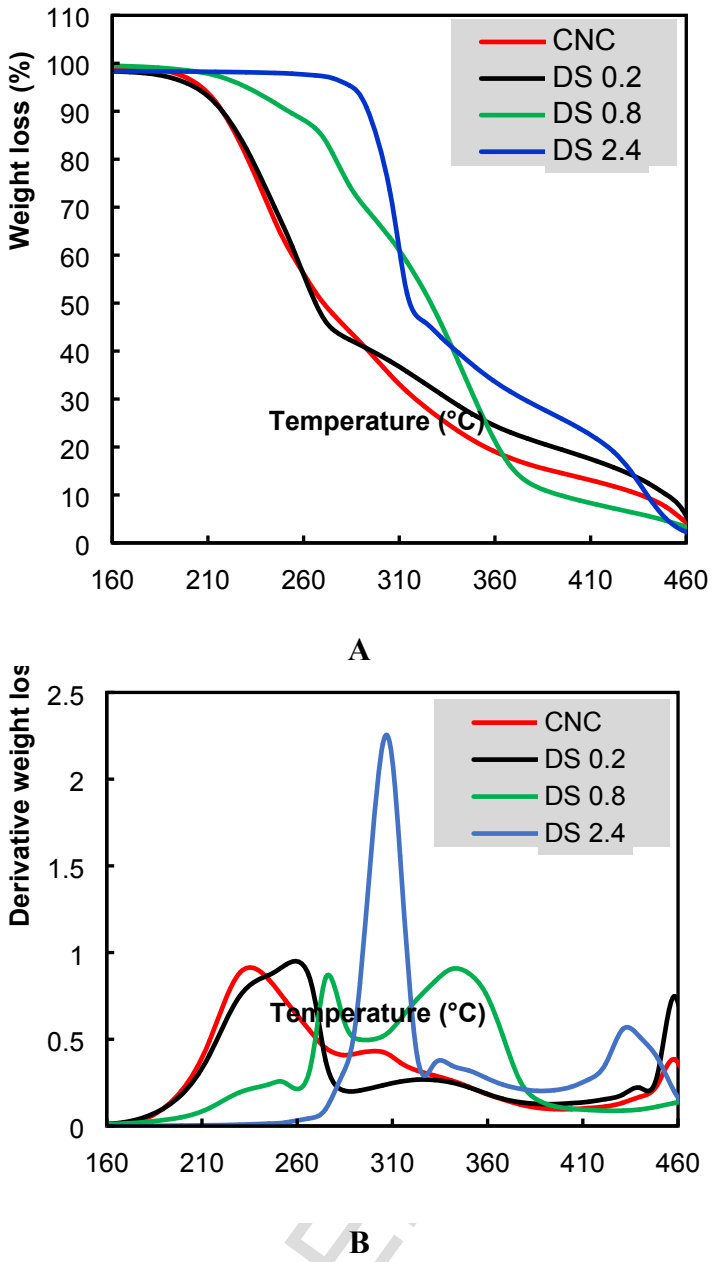

Figure 5. TGA thermograms (a) and derivative weight loss (b) of native and modified CNC samples.

3.6. Epoxy – CNC nanocomposites

In this study, nanocomposites of an epoxy resin were produced by the reaction of a difunctional diglycidyl ether of bisphenol A with an epoxide equivalent weight of 172 – 185 g/eq

and a polyetheramine (average M_n 230g/mol) curing agent in the presence of native and modified CNC. Grafting of medium aliphatic chains in place of hydroxyl functional groups of CNC resulted in reduction of intra- and intermolecular hydrogen bonding among the CNC particles. Also, the grafted bulky pendant aliphatic fatty acid on the cellulose crystals limits the aggregation and agglomeration of CNCs [39]. This prompted in an improvement in the dispersability of CNC in non-polar solvents (Figure 4). Figure 6 (a, b and c) showed the dispersion of native and modified (DS 0.2) CNC in epoxy resins at 2.5% and 5 wt.% after homogenization. While the native samples (2.5%) formed a cloudy dispersion, the modified samples resulted in an almost transparent dispersion indicating excellent dispersability with no or limited aggregation. The impact of CNC modification on the mechanical and thermal properties of epoxy thermoset systems were studied here to demonstrate the reinforcing potential of such modifications in polymer nanocomposites applications.

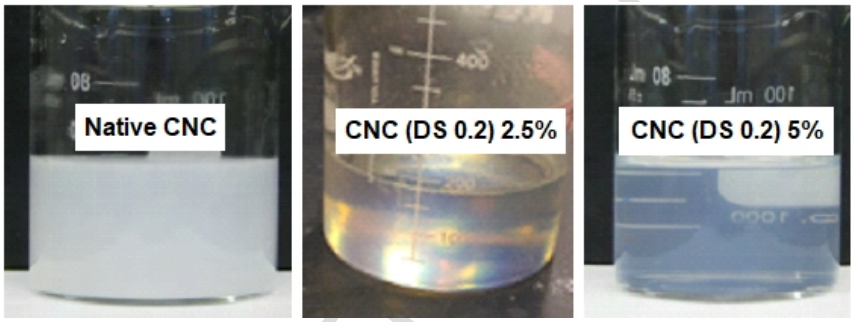

a b c

Figure 6. Photograph of the dispersion of CNC in epoxy (a) native CNC dispersed in epoxy at 2.5% concentration, (b) modified CNC (DS 0.8) dispersed in epoxy at a concentration of 2.5%, and (c) modified CNC (DS 0.8) dispersed in epoxy at a concentration of 5%.

3.6.1. Effect of CNC modifications on mechanical properties of epoxy

Epoxy nanocomposites loaded with CNC (native and modified) at 2.5% and 5% concentration were evaluated to understand the effect of modification on its reinforcing potential.

Figure 6 (a and b) presented the tensile strength of the nanocomposites at maximum load on tensile dog bone sample specimens. While native CNC had a clear reinforcing effect, the lightly and intermediately modified CNCs exhibited exceedingly remarkable reinforcing effect as observed from the tensile strength and modulus improvement of the epoxy nanocomposites (Figure 6a and b), pointing an effective load transfer from the matrix to the fillers. The reason for the outstanding load transfer and reinforcement of the modified CNC as compared to native CNC based nanocomposites were due to the nanodispersion of esterified CNC particles in the epoxy matrix in conjuncture with a possibility of intimate interaction between the epoxy matrix and the nanoparticles that led to high stress transfer. Abraham *et al* [39] observed similar trend of load transfer improvement by using a hydrophobic CNC (acetylated) in epoxy nanocomposites. It was interesting to notice that the intermediately modified CNC (DS 0.8) caused a similar reinforcing effect as that of the lightly modified CNC (DS 0.2) as shown in Figure 7. Although a DS of 0.8 CNC meant that the modification attacked the crystalline structure, as it is significantly higher than the stipulated DS 0.3 for surface modification, it is plausible that the core of the crystalline structure stayed intact and only partial swelling and delamination that exposed more –OH groups has occurred as observed in the XRD result (Figure 2) [33,40]. The loss of some crystallinity because of the partial delamination was expected to result in lower reinforcing effect of epoxy as compared to the lightly modified CNC (DS 0.2). However, as presented in Figure 7, the two levels of modifications exhibited similar reinforcing effect. It is worth to mention that the higher degree of lauric acid grafting in the DS 0.8 as compared to the DS 0.2 resulted in higher hydrophobicity (as shown in Figure 3), making it more compatible with the low ionic strength epoxy matrix. Thus, despite losing some crystalinity with the partial delamination, a compensation by a higher hydrophobicity by such modifications (DS 0.8) could promote an

enhanced compatibility and interfacial interaction that resulted in the observed excellent reinforcing effect.

On the contrary, the highly modified CNC (DS 2.4) did not show reinforcing effect. This is not a surprise, as the high modification destroyed the crystallinity (Figure 2) that is responsible for the extraordinary strength of CNCs. Elongation at break results from the stress – strain study (Figure 6b) showed that loading of CNC (DS 2.4) at 2.5 %, and 5 % resulted in an increase in elongation of 25.1 % and 34.3%, respectively. This clearly indicated that the presence of a significant long aliphatic chains grafted on the CNC as in the DS 2.4 samples have plasticized the epoxy network. While the elongation at break of native CNC reinforced epoxy nanocomposites have marginally reduced as compared to the neat epoxy matrix, the esterified CNC at low substitution (DS 0.2 and DS 0.8) did not change the elasticity significantly (analysis of variance $P > 0.05$).

We compared the experimental elastic modulus with those predicted by the Halpin-Tsai model that is commonly used for estimation of nanocomposite mechanical properties. The Halpin-Tsai model is a widely accepted semi-empirical equation for prediction of the modulus of a discontinuous composite structures [9,41,42]. The model is based on the assumptions that only the matrix sustains the axial load and transmits stress to the fiber through shear stress and that all fibers are well dispersed in the matrix. The theoretical calculated moduli (*Eo*) of the composites for randomly oriented fiber fillers can be computed using the following equation (3)[43,44].

$$E_o = \frac{3}{8}E_L + \frac{5}{8}E_T \quad (3)$$

Where E_L and E_T are the longitudinal and transverse Young's modulus of unidirectional composites, respectively. These can be estimated using equations (4) and (5).

$$E_L = \frac{1 + 2(l_f/d_f)\eta_L V_f}{1 - \eta_T V_f} E_m \quad (4)$$

$$E_T = \frac{1 + 2\eta_L V_f}{1 - \eta_T V_f} E_m \quad (5)$$

And,

$$\eta_L = \frac{(E_{fL}/E_m) - 1}{(E_{fL}/E_m) + 2(l_f/w_f)} \quad (6)$$

$$\eta_T = \frac{(E_{fL}/E_m) - 1}{(E_{fL}/E_m) + 2} \quad (7)$$

Where, E_o is the predicted modulus of the composite, E_m is the modulus of the neat epoxy matrix, E_{fL} and E_{fT} are the longitudinal and transverse Young's modulus of the CNC filler. l_f and w_f are the length and width of the CNC, respectively. For CNC in our study, E_{fL}, E_{fT}, and l_f/d_f of 143 GPa [45], 24.8 GPa [44], 20 [46], respectively were used. V_f is the volume fraction of the CNC filler in the epoxy matrix. Based on Halpin-Tsai model (equation 3), the theoretical moduli of the nanocomposite were 3.7 GPa and 3.9 GPa for the 2.5 % and 5 % CNC based nanocomposites. These modulus values are in excellent agreement with the modulus obtained for the CNC DS 0.2 nanocomposite, *i.e.* 3.6 and 3.9 GPa at 2.5 % and 5 % loading, respectively. Since the Halpin – Tsai model assumes that the nanoparticle is well dispersed, the result obtained here pointed out that the lightly modified CNC (DS 0.2) was the most efficient reinforcing agent in line with the other observations.

Overall, the mechanical property testing elucidated that there was good compatibility and as a result effective stress transfer from the epoxy matrix to the lauric acid modified CNCs (DS 0.2,

0.8). Highly esterified CNC (DS 2.4) showed poor promise as a reinforcing filler of rigid structures as it did not improve the tensile strength or modulus as compared to the neat epoxy baseline matrix. However, it is worth to mention here that it caused significant increase in the elasticity without changing the tensile strength, pointing that it could have a toughing effect. Since epoxy in general is a brittle material, some practical applications can benefit from such toughing additives.

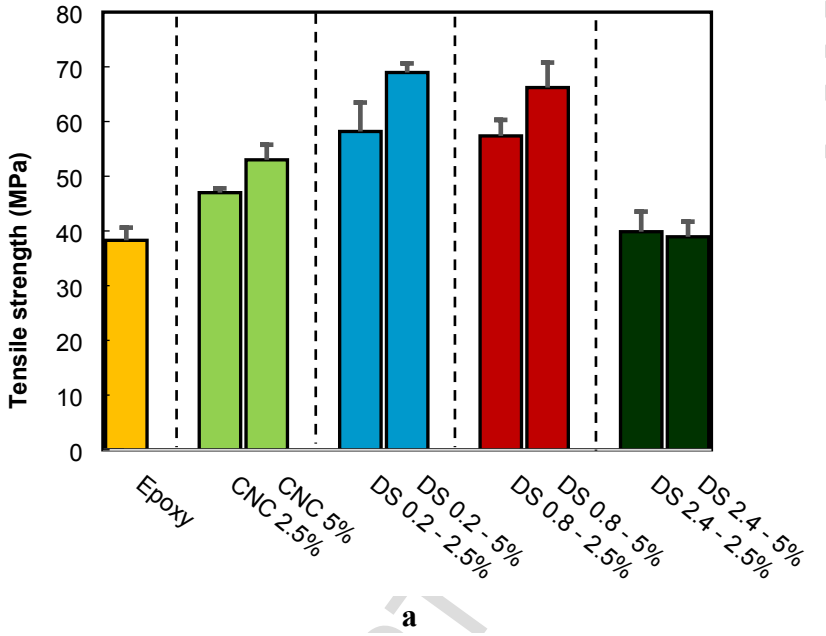

a

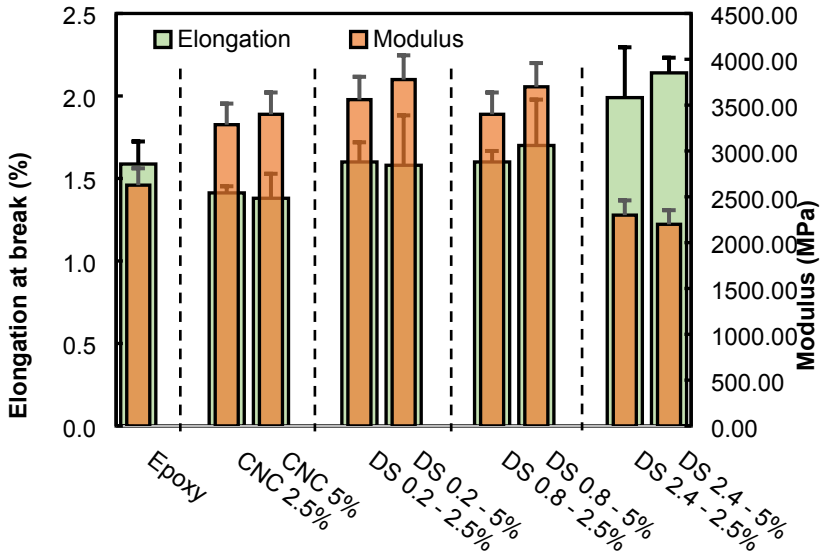

b

Figure 7. Mechanical properties of neat epoxy, and nanocomposites reinforced with native CNC, and esterified CNC (DS 0.2, 0.8 and 2.4). (a) Tensile strength, (b) Modulus and elongation at break.

3.6.2. Dynamic Mechanical analysis

The thermo-mechanical properties of neat epoxy, and epoxy nanocomposites reinforced with native and modified CNCs were tested by DMA to evaluate their mechanical properties at different temperatures. The variation in the storage modulus (E') and loss modulus (E'') of the neat epoxy and the nanocomposites as a function of temperature are presented in Figure 8 (a and b). It was evident that below T_g all nanocomposite formulations exhibited higher modulus than the pure epoxy matrix pointing to the efficient stress transfer from the matrix to the CNC. This included even the highly modified CNC (DS 2.4) at both 2.5% and 5%. The reason for this was that the presence of fillers in general restrict chain mobility that led to the observed enhancement in modulus [47]. An increase in filler loading imparts additional mobility constraints that result in higher storage modulus. This is in line with the tensile modulus observations.

As shown in Figure 8b and Table 2, the nanocomposites with CNC DS 0.2 at 2.5 % and 5 % concentrations exhibited their peak loss modulus (E'') values at higher temperature than the epoxy matrix. This is because of a strong interfacial adhesion between the epoxy and the esterified CNC. The highly modified CNC (DS 2.4) based composites displayed their maximum E'' at the lowest temperature in comparison with the other composites or the neat epoxy. This is an indication of the reduction of glass transition temperature (T_g) of these nanocomposites due to the plasticization effect of the aliphatic fatty acids that are grafted on the CNC. These observations were consistent with the other mechanical property results. In general, the use of

native CNC and surface modified CNCs improved the T_g. The results obtained from differential scanning calorimetry (DSC) illustrated a similar trend to those from DMA (Table 2).

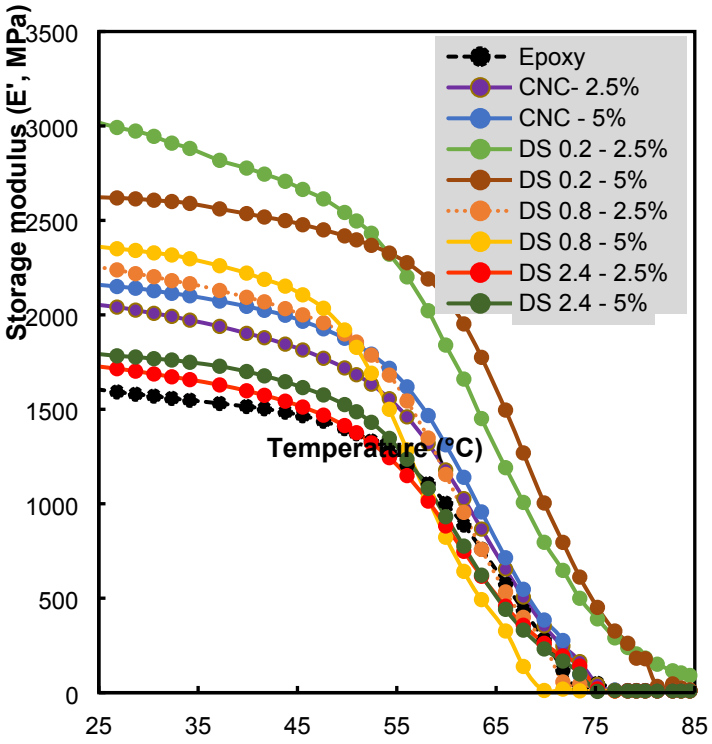

a

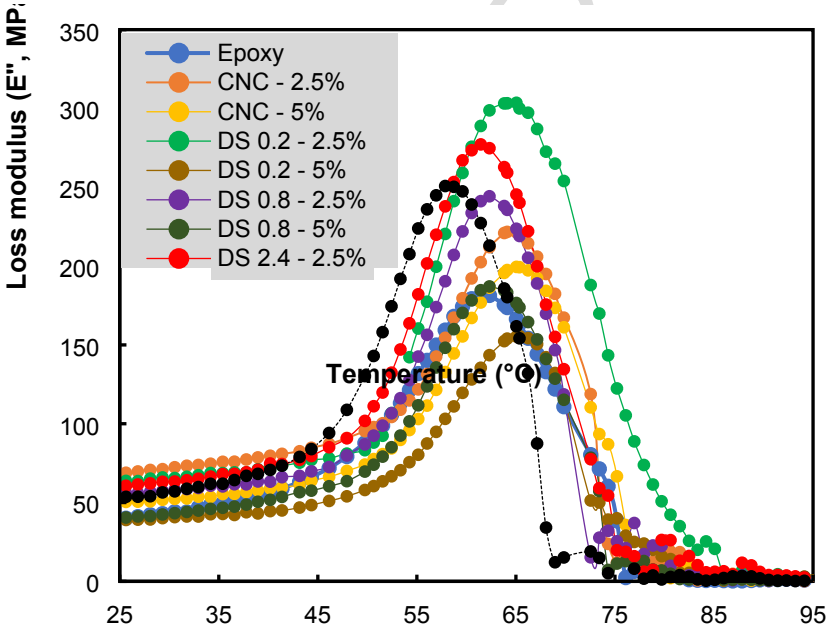

b

Figure 8. Dynamic mechanical properties of neat epoxy matrix and their composites with native and modified CNC (a) Storage modulus, (b) Loss modulus.

Table 2. Summary glass transition temperatures, storage tensile moduli (E′) from DMA, T_g (from DSC analysis, E″ peak temperatures), and of neat epoxy and epoxy/CNC nanocomposites as a function of CNC modification and content.

Sample	**Filler content**	**DMA**			**DSC**
	(%)	***E′* at 30 °C (MPa)**	***E′* at 80 °C (MPa)**	***T_g* by max *E″* (°C)**	***T_g* (°C)**
Epoxy	-	1570	48	60	49
Epoxy CNC	2.5	2008	93	64	51
Epoxy CNC	5	2128	109	65	56
Epoxy CNC DS 0.2	2.5	2948	390	65	58
Epoxy CNC DS 0.2	5	2607	451	66	58
Epoxy CNC DS 0.8	2.5	2202	59	62	59
Epoxy CNC DS 0.8	5	2328	51	62	58
Epoxy CNC DS 2.4	2.5	1687	29	62	55
Epoxy CNC DS 2.4	5	1768	18	58	53

3.6.3. Scanning electron microscope (SEM)

The tensile fracture surface morphologies of the nanocomposites were further characterized by scanning electron microscopy (SEM), and images are displayed in Figure 9. The neat epoxy displayed a very smooth fracture surface, and almost no marks were observed due to the brittleness of the matrix. After the incorporation of CNC (native and modified), clear markings were observed on the fracture surface. In all the nanocomposites, no major aggregation and agglomeration was observed. Overall, the CNC fillers appear to be well individualized and

coated with the epoxy matrix. The low loading level, coupled with the intense homogenization of the CNC (unmodified and modified) in the epoxy prior to curing could have assisted with the dispersion. The holes (marked by the arrows) indicate the pullout of CNC during the tensile fracture. This is indicative of good interfacial bonding between the epoxy matrix and the fillers. In the esterified CNC fillers, hydrogen bonding between the carbonyl group of the ester and the residual amines could have caused the strong interaction.

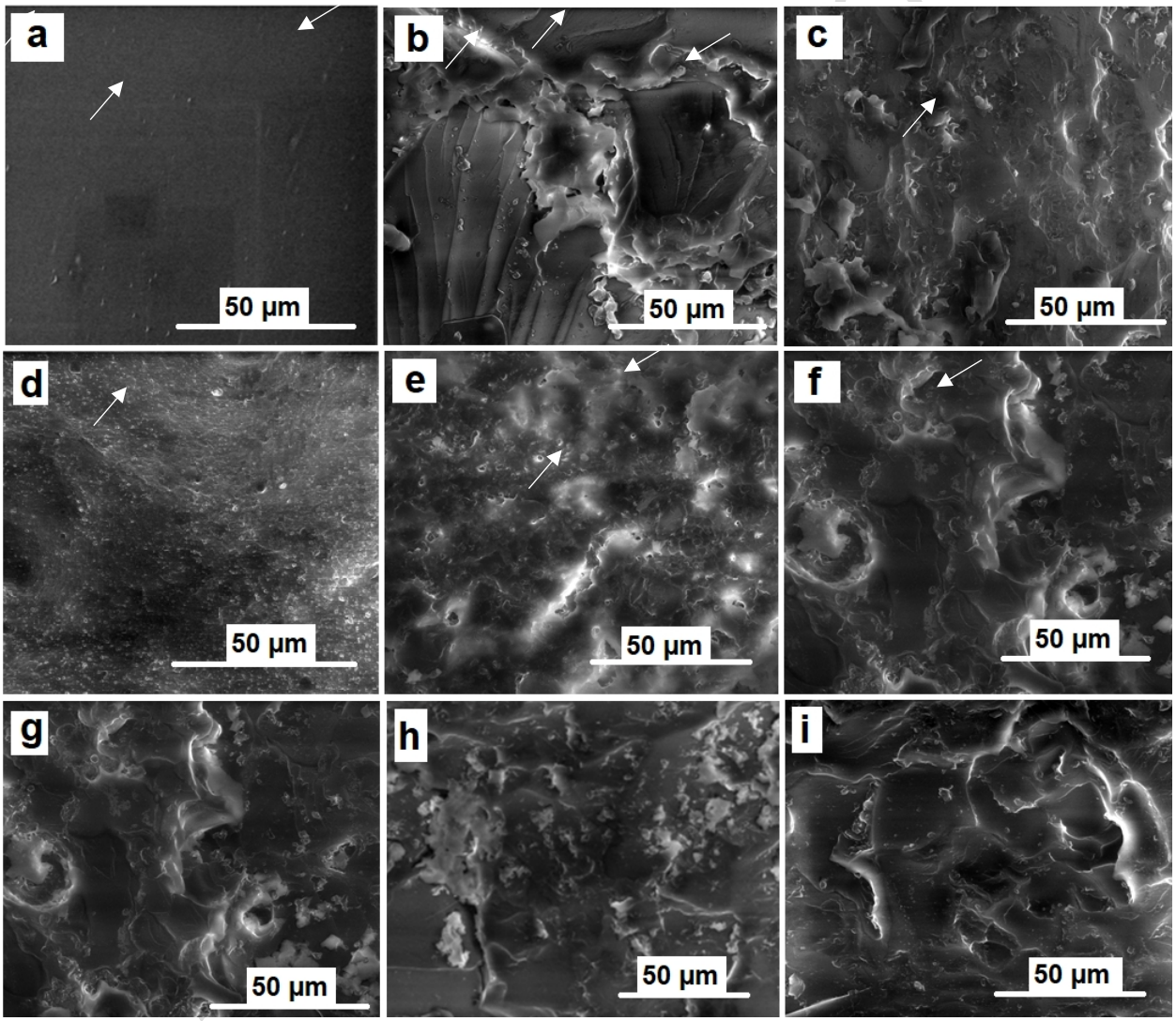

Figure 9. SEM images of the fractured surfaces of (a) the neat epoxy resin; (b) native CNC – epoxy composite (2.5 % filler content), (c) native CNC – epoxy composite (5 % filler content), (d) CNC DS 0.2 – epoxy composite (2.5 % filler content), (e) CNC DS 0.2 – epoxy composite (5 % filler content), (f) CNC DS 0.8 – epoxy composite (2.5 % filler content), (g) CNC DS 0.8 –

epoxy composite (5 % filler content), (h) CNC DS 2.4 – epoxy composite (2.5 % filler content), (i) CNC DS 2.4 – epoxy composite (5 % filler content).

3.6.4. Water uptake studies

Water absorption in epoxy based materials has been a subject of study in many researches [48–51] for the outstanding properties of epoxy materials could be immensely affected by the water absorbed and thus its potential use in structural applications can be constrained. For instance, a substantial change in T_g, tensile strength, modulus, toughness, crack resistance, adhesion strength of epoxy materials has been reported as a result of moisture uptake [51–53]. Combining an inherently hydrophilic material, such as CNC as a reinforcing agent could worsen the moisture uptake and negatively affect the nanocomposite properties [54]. Hydrophobic modification of CNC could potentially mitigate this grand challenge. The study here has targeted on how the incorporation of native and fatty acid modified CNC affects the water uptake behavior of the epoxy composites over a short period.

Water absorption patter of the neat epoxy and the nanocomposites with native and modified CNC over a period of seven days is presented in Figure 10. All sample specimens appeared to uptake a significant moisture in the first three days. While the absorption rate seemed to reduce afterwards, equilibration was not achieved over the studied period include the baseline epoxy. This is in agreement with Chow [48], which showed that epoxy's moisture absorption saturated with 2.3% moisture absorption after it was subjected to water testing for 35 days. Since water sorption is dependent on the presence of free volume in polymer matrices [55], the incorporation of nanoparticles can generally reduce the uptake by occupying the available space. However, the type and concentration of functional moieties of the nanoparticle is critical in deterring moisture uptake. The use of native CNC and lightly modified CNC (DS 0.2) exhibited more absorption

than the neat epoxy matrix at both 2.5% and 5% concentration ranges. On the contrary, higher levels of fatty acid grafting on the CNC clearly improved the water uptake as compared to the unmodified or lightly modified CNC fillers. As expected, nanocomposites filled with the highly modified CNC (DS 2.4) displayed a reduced moisture uptake. A more pronounced reduction in moisture absorption was observed for nancomposites that were filled with 5% loading of such CNC. The replacement of the –OH functionalities with hydrophobic fatty acids clearly made it hydrophobic as described in the previous section. It appeared here that the hydrophobicity of these CNC (DS 2.4) were carried to the epoxy nanocomposite to cause the observed reduction of moisture uptake.

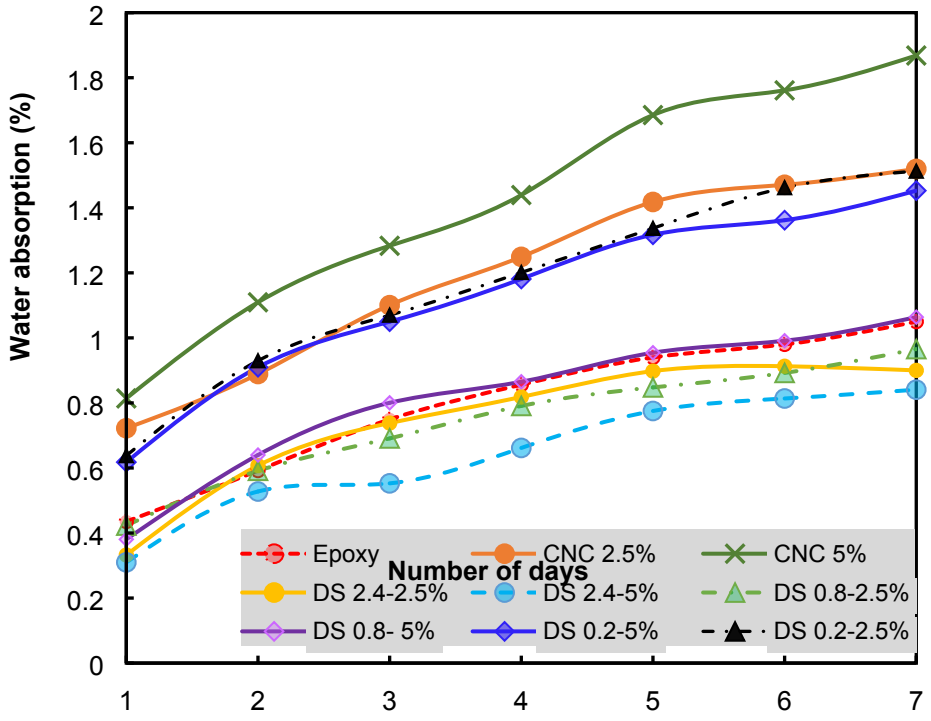

Figure 10. Short term water absorption of neat epoxy and epoxy composites with native and modified CNC.

4. Conclusions

In this study, the replacement of –OH functional groups of CNC with fatty acids was conducted via grafting lauric acid using a one step process to promote hydrophobicity, improve its dispersion, and increase interfacial adhesion with epoxy. Overall, the grafting of the lauric acid on the CNC altered the thermal stability, polarity and thus the dispersability at various degrees depending on the level of grafting. Native CNC and three types of CNCs with various degrees of grafted acid were incorporated into an epoxy matrix via a solvent-free route. The lightly modified CNCs (DS 0.2 and 0.8) resulted in an impressive reinforcing effect in epoxy that was demonstrated by an increase in the tensile strength and modulus. The tensile strength and modulus of the baseline epoxy was improved by 77% and 44%, respectively by incorporating 5% CNC (DS 0.2). Such materials could have important implications for the manufacture of printed circuit boards, structural composites and adhesives. Highly modified CNC with a DS of 2.4 clearly lost its crystalline structure. However, because of the plasticizing effect of the fatty acid it caused an overall improvement in toughness, demonstrated by increase in elongation by up to 35%, without a significant change in tensile strength, and a reduced water uptake of the epoxy nanocomposites.

Acknowledgements

We acknowledge Celluforce Inc. for supplying free CNC samples. T. Mekonnen acknowledges the Department of Chemical Engineering and the Faculty of Engineering of the University of Waterloo for their start-up funding. We would like to thank the technical support of Dr. Geoff Rivers, Mingqian (John) Zhang, Ralph Dickout, Ewomazino Ojogbo, and Rachel Blanchard.

References

[1] S.A. Xu, G.T. Wang, Y.W. Mai, Effect of hybridization of liquid rubber and nanosilica particles on the morphology, mechanical properties, and fracture toughness of epoxy composites, J. Mater. Sci. 48 (2013) 3546–3556. doi:10.1007/s10853-013-7149-4.

[2] Acmite Market Intelligence, Global Epoxy Resin Market, Ratingen, Germany, 2014. http://www.acmite.com.

[3] Y.T. Park, Y. Qian, C. Chan, T. Suh, M.G. Nejhad, C.W. Macosko, A. Stein, Epoxy toughening with low graphene loading, Adv. Funct. Mater. 25 (2015) 575–585. doi:10.1002/adfm.201402553.

[4] N. Domun, H., Improving the fracture toughness and the strength of epoxy using nanomaterials a review of the current status, Nanoscale. 7 (2015) 10294–10329. doi:10.1039/c5nr01354b.

[5] H.M. Naguib, M.A. Ahmed, Z.L. Abo-Shanab, Silane coupling agent for enhanced epoxy-iron oxide nanocomposite, J. Mater. Res. Technol. 7 (2018) 21–28. doi:10.1016/j.jmrt.2017.03.002.

[6] J.A.M. Ferreira, L.P. Borrego, J.D.M. Costa, C. Capela, Fatigue behaviour of nanoclay reinforced epoxy resin composites, Compos. Part B Eng. 52 (2013) 286–291. doi:10.1016/j.compositesb.2013.04.003.

[7] K. Zhang, L. Wang, F. Wang, G. Wang, Z. Li, Preparation and characterization of modified-clay-reinforced and toughened epoxy-resin nanocomposites, J. Appl. Polym. Sci. 91 (2004) 2649–2652. doi:10.1002/app.13445.

[8] Y. Yan, J. Cui, S. Zhao, J. Zhang, J. Liu, J. Cheng, Interface molecular engineering of single-walled carbon nanotube/epoxy composites, J. Mater. Chem. 22 (2012) 1928–1936. doi:10.1039/C1JM14310G.

[9] J. Townsend, R. Burtovyy, P. Aprelev, K.G. Kornev, I. Luzinov, Enhancing Mechanical and Thermal Properties of Epoxy Nanocomposites via Alignment of Magnetized SiC Whiskers, ACS Appl. Mater. Interfaces. 9 (2017) 22927–22940. doi:10.1021/acsami.7b04546.

[10] B. Vollick, P.-Y. Kuo, H. Thérien-Aubin, N. Yan, E. Kumacheva, Composite Cholesteric Nanocellulose Films with Enhanced Mechanical Properties, Chem. Mater. 29 (2017) 789–795. doi:10.1021/acs.chemmater.6b04780.

[11] M. Bhattacharya, Polymer Nanocomposites-A Comparison between Carbon Nanotubes, Graphene, and Clay as Nanofillers, Materials (Basel). 9 (2016) 262 - 297. doi:10.3390/ma9040262.

[12] K. Muller, B., Review on the Processing and Properties of Polymer Nanocomposites and Nanocoatings and Their Applications in the Packaging, Automotive and Solar Energy Fields, Nanomaterials. 7 (2017). doi:10.3390/nano7040074.

[13] K. Wakabayashi, P.J. Brunner, J. Masuda, S.A. Hewlett, J.M. Torkelson, Polypropylene-graphite nanocomposites made by solid-state shear pulverization: Effects of significantly exfoliated, unmodified graphite content on physical, mechanical and electrical properties, Polymer (Guildf). 51 (2010) 5525–5531. doi:10.1016/j.polymer.2010.09.007.

[14] B.M. Cromer, E.B. Coughlin, A.J. Lesser, Evaluation of a new processing method for improved nanocomposite dispersions, Nanocomposites. 1 (2015) 152–159. doi:10.1179/2055033215Y.0000000009.

[15] Z. Hu, R.M. Berry, R. Pelton, E.D. Cranston, One-Pot Water-Based Hydrophobic Surface Modification of Cellulose Nanocrystals Using Plant Polyphenols, ACS Sustain. Chem. Eng. 5 (2017) 5018–5026. doi:10.1021/acssuschemeng.7b00415.

[16] S.X. Peng, H. Chang, S. Kumar, R.J. Moon, J.P. Youngblood, A comparative guide to controlled hydrophobization of cellulose nanocrystals via surface esterification, Cellulose. 23 (2016) 1825–1846. doi:10.1007/s10570-016-0912-3.

[17] K.H.M. Kan, J. Li, K. Wijesekera, E.D. Cranston, Polymer-Grafted Cellulose Nanocrystals as pH-Responsive Reversible Flocculants, Biomacromolecules. 14 (2013) 3130–3139. doi:10.1021/bm400752k.

[18] A. Boujemaoui, C. Cobo Sanchez, J. Engström, C. Bruce, L. Fogelström, A. Carlmark, E. Malmström, Polycaprolactone Nanocomposites Reinforced with Cellulose Nanocrystals Surface-Modified via Covalent Grafting or Physisorption: A Comparative Study, ACS Appl. Mater. Interfaces. 9 (2017) 35305–35318. doi:10.1021/acsami.7b09009.

[19] Y. Habibi, Key advances in the chemical modification of nanocelluloses, Chem. Soc. Rev. 43 (2014) 1519–1542. doi:10.1039/C3CS60204D.

[20] J. Bras, C. Vaca-Garcia, M.-E. Borredon, W. Glasser, Oxygen and water vapor permeability of fully substituted long chain cellulose esters (LCCE), Cellulose. 14 (2007) 367–374. doi:10.1007/s10570-007-9123-2.

[21] L. Timhadjelt, A. Serier, M.N. Belgacem, J. Bras, Elaboration of cellulose based nanobiocomposite: Effect of cellulose nanocrystals surface treatment and interface “ melting,” Ind. Crop. Prod. 72 (2015) 7–15. doi:10.1016/j.indcrop.2015.02.040.

[22] B.M.E. Vaca-Garcia, Determination of the degree of substitution (DS) of mixed cellulose esters by elemental analysis, Cellulose. 8 (2001) 225–231. doi:10.1023/A:1013133921626.

[23] S. Eyley, W. Thielemans, Surface modification of cellulose nanocrystals, Nanoscale. 6 (2014) 7764–7779. doi:10.1039/C4NR01756K.

[24] I. Cumpstey, Chemical Modification of Polysaccharides, ISRN Org. Chem. 2013 (2013) 1–27. doi:10.1155/2013/417672.

[25] A. Junior de Menezes, G. Siqueira, A.A.S. Curvelo, A. Dufresne, Extrusion and characterization of functionalized cellulose whiskers reinforced polyethylene nanocomposites, Polymer (Guildf). 50 (2009) 4552–4563. doi:10.1016/j.polymer.2009.07.038.

[26] S. Kumari, G.S. Chauhan, New cellulose-lysine Schiff-base-based sensor-adsorbent for mercury ions, ACS Appl. Mater. Interfaces. 6 (2014) 5908–5917. doi:10.1021/am500820n.

[27] M. Zaman, H. Xiao, F. Chibante, Y. Ni, Synthesis and characterization of cationically modified nanocrystalline cellulose, Carbohydr. Polym. 89 (2012) 163–170. doi:10.1016/j.carbpol.2012.02.066.

[28] M.-C. Li, Q. Wu, K. Song, S. Lee, Y. Qing, Y. Wu, Cellulose Nanoparticles: Structure–Morphology–Rheology Relationships, ACS Sustain. Chem. Eng. 3 (2015) 821–832. doi:10.1021/acssuschemeng.5b00144.

[29] L. Du, J. Wang, Y. Zhang, C. Qi, M. Wolcott, Z. Yu, Preparation and Characterization of Cellulose Nanocrystals from the Bio-ethanol Residuals, Nanomaterials. 7 (2017) 51 - 63. doi:10.3390/nano7030051.

[30] M. Okamura, K., Shiraishi, N., Norimoto, Change of X-ray diffraction peaks in aliphatic cellulose ester homologues, Wood Res. 69 (1983). 1-5.

[31] W. Kong, X. Fu, Y. Yuan, Z. Liu, J. Lei, Preparation and thermal properties of crosslinked polyurethane/lauric acid composites as novel form stable phase change materials with a low degree of supercooling, RSC Adv. 7 (2017) 29554–29562. doi:10.1039/C7RA04504B.

[32] S. Farris, L. Introzzi, P. Biagioni, T. Holz, A. Schiraldi, L. Piergiovanni, Wetting of Biopolymer Coatings: Contact Angle Kinetics and Image Analysis Investigation, Langmuir. 27 (2011) 7563–7574. doi:10.1021/la2017006.

[33] E. Espino-Pérez, S. Domenek, N. Belgacem, C. Sillard, J. Bras, Green Process for Chemical Functionalization of Nanocellulose with Carboxylic Acids, Biomacromolecules. 15 (2014) 4551–4560. doi:10.1021/bm5013458.

[34] A. Ferreira, V. Alves, I. Coelhoso, Polysaccharide- Based Membranes in Food Packaging Applications, Membranes (Basel). 6 (2016) 22. doi:10.3390/membranes6020022.

[35] L. Tang, C. Weder, Cellulose Whisker/Epoxy Resin Nanocomposites, ACS Appl. Mater. Interfaces. 2 (2010) 1073–1080. doi:10.1021/am900830h.

[36] F. Ansari, S. Galland, M. Johansson, C.J.G. Plummer, L.A. Berglund, Cellulose nanofiber network for moisture stable, strong and ductile biocomposites and increased epoxy curing rate, Compos. Part A Appl. Sci. Manuf. 63 (2014) 35–44. doi:10.1016/j.compositesa.2014.03.017.

[37] A.P. Schniewind, No Concise Encyclopedia of Wood and Wood Based MaterialsTitle, 1st ed., Pergamon Press, Oxford, UK 1989.

[38] N. Yildirim, S. Shaler, A Study on Thermal and Nanomechanical Performance of Cellulose Nanomaterials (CNs), Materials (Basel). 10 (2017) 718. doi:10.3390/ma10070718.

[39] E. Abraham, D. Kam, Y. Nevo, R. Slattegard, A. Rivkin, S. Lapidot, O. Shoseyov, Highly Modified Cellulose Nanocrystals and Formation of Epoxy-Nanocrystalline Cellulose

(CNC) Nanocomposites, ACS Appl. Mater. Interfaces. 8 (2016) 28086–28095. doi:10.1021/acsami.6b09852.

[40] E. Ojogbo, R. Blanchard, T. Mekonnen, Hydrophobic and Melt Processable Starch-Laurate Graft Polymers: Synthesis, Structure – Property Correlations, J. Polym. Sci. Part A-Polymer Chem. (2018). doi: 10.1002/pola.20180436

[41] J.C.H. Affdl, J.L. Kardos, The Halpin-Tsai equations: A review, Polym. Eng. Sci. 16 (1976) 344–352. doi:10.1002/pen.760160512.

[42] R. Libanori, R.M. Erb, A.R. Studart, Mechanics of Platelet-Reinforced Composites Assembled Using Mechanical and Magnetic Stimuli, ACS Appl. Mater. Interfaces. 5 (2013) 10794–10805. doi:10.1021/am402975a.

[43] L.E. Nielsen, R.F. Landel, Mechanical properties of polymers and composites, M. Dekker, 1994. http://primo.tug-libraries.on.ca/primo_library/libweb/action/PushToAction.do?indx=1&doc=vtug1188431&recId=vtug1188431&docs=vtug1188431&pushToType=Mendeley&fromEshelf=false&vid=WATERLOO&fromMendeley=true&fromSitemap=1&afterPDS=true (accessed May 6, 2018).

[44] X. Miao, F. Tian, J. Lin, H. Li, X. Li, F. Bian, X. Zhang, Tuning the mechanical properties of cellulose nanofibrils reinforced polyvinyl alcohol composites via altering the cellulose polymorphs, RSC Adv. 6 (2016) 83356–83365. doi:10.1039/C6RA14517E.

[45] A. Šturcová, G.R. Davies, S.J. Eichhorn, Elastic Modulus and Stress-Transfer Properties of Tunicate Cellulose Whiskers, Biomacromolecules. 6 (2005) 1055–1061. doi:10.1021/bm049291k.

[46] CelluForce Inc., The core properties of CelluForce NCC, (2018). http://www.celluforce.com/en/products/core-properties/ (accessed May 6, 2018).

[47] A. Kiziltas, B. Nazari, D. Gardner, D. Bousfield, Polyamide 6- cellulose composites: effect of cellulose composition on melt rheology and crystallization behavior.(Report), Polym. Eng. Sci. 54 (2014) 739. doi:10.1002/pen.23603.

[48] W.S. Chow, Water absorption of epoxy/glass fiber/organo-montmorillonite nanocomposites, Express Polym. Lett. 1 (2007) 104–108. doi:10.3144/expresspolymlett.2007.18.

[49] H. Alamri, I.M. Low, Mechanical properties and water absorption behaviour of recycled cellulose fibre reinforced epoxy composites, Polym. Test. 31 (2012) 620–628. doi:10.1016/j.polymertesting.2012.04.002.

[50] Y. Takeshita, E. Becker, S. Sakata, T. Miwa, T. Sawada, States of water absorbed in water-borne urethane/epoxy coatings, Polymer (Guildf). 55 (2014) 2505–2513. doi:10.1016/j.polymer.2014.03.027.

[51] L.W. Jelinski, J.J. Dumais, A.L. Cholli, T.S. Ellis, F.E. Karasz, Nature of the water-epoxy interaction, Macromolecules. 18 (1985) 1091–1095. doi:10.1021/ma00148a008.

[52] I. Blanco, G. Cicala, M. Costa, A. Recca, Development of an epoxy system characterized

by low water absorption and high thermomechanical performances, J. Appl. Polym. Sci. 100 (2006) 4880–4887. doi:10.1002/app.23276.

[53] L. Li, S. Zhang, Y. Chen, M. Liu, Y. Ding, X. Luo, Z. Pu, W. Zhou, S. Li, Water Transportation in Epoxy Resin, Chem. Mater. 17 (2005) 839–845. doi:10.1021/cm048884z.

[54] T. Mekonnen, P. Mussone, K. Alemaskin, L. Sopkow, J. Wolodko, P. Choi, D. Bressler, Biocomposites from hydrolyzed waste proteinaceous biomass: mechanical, thermal and moisture absorption performances, J. Mater. Chem. A. 1 (2013) 13186. doi:10.1039/c3ta13560h.

[55] O. Becker, R.J. Varley, G.P. Simon, Thermal stability and water uptake of high performance epoxy layered silicate nanocomposites, Eur. Polym. J. 40 (2004) 187–195. doi:10.1016/j.eurpolymj.2003.09.008.

Highlights

- Heterogeneous esterification of CNC with an activated fatty acid induced hydrophobicity of CNCs
- The crystallinity, dispersability, and thermal stability of CNCs was altered with the modification.
- Lightly modified CNC resulted in excellent reinforcement of epoxy resins
- Water absorption of epoxy nanocomposites diminished with the hydrophobic CNC